11th Australasian Fluid Mechanics Conference
University of Tasmania, Hobart, Australia
14-18 December 1992

FLOW VISUALISATION IN A CARDIAC ASSIST DEVICE

Allen H. NUGENT[1], Christopher D. BERTRAM[1], Chun-xiu YE[2] and Mitsuo UMEZU[3]

[1]Centre for Biomedical Engineering, University of New South Wales, Kensington, NSW 2033, AUSTRALIA

[2]Cardiac Prostheses Research Laboratory, St Vincent's Hospital, Sydney, AUSTRALIA

[3]Department of Mechanical Engineering, Waseda University, Tokyo, JAPAN

ABSTRACT

The Spiral Vortex (SV) ventricular assist device (VAD), a pulsatile blood pump that was designed to minimise trauma to red blood cells through optimisation of relevant fluid dynamic parameters, has been evaluated using flow visualisation techniques. Qualitative and quantitative data has been obtained on velocity distribution, shear stress, turbulence, and flow recirculation, during key phases in the pump cycle. In comparison to a VAD of conventional design, the SV exhibits less turbulence, less recirculation, and better washout of critical surfaces.

GLOSSARY

diastole	the filling phase of the pump cycle
haemolysis	lysing of red blood cells (erythrocytes) and platelets
systole	the ejection phase of the pump cycle
thrombosis	deposition of fibrin and platelets by coagulation mechanisms

INTRODUCTION

Ventricular assist devices have been successfully used to support the failing heart in patients with reversible (ie. following myocardial infarction and/or surgery) and irreversible (ie. awaiting a donor heart for transplantation) heart failure. However, these devices continue to be plagued by complications associated with surface-chemical and fluid-dynamic interactions between the pump and the blood, namely, thrombosis, thromboembolism, and bleeding (Farrar et al, 1988). Prior to this project, no group seems to have specifically aimed at reducing these complications through improved fluid mechanics. The Spiral Vortex VAD was designed to address this problem.

The SV VAD is conventional in that it consists of a pneumatically actuated diaphragm and valved conduits, using segmented polyether-polyurethane (TM5, Toyobo Co., Japan) for the blood contacting surfaces (including the diaphragm). However, it is unconventional in that it features a sigmoid-conical pump chamber, with non-coplanar inflow and outflow conduits; the outlet is located at the apex and is axially-oriented, whereas the inlet is tangentially-located and intersects the equatorial plane at 45° to the vertical (Fig. 1).

The hydraulic performance of the VAD, which has been previously investigated (Umezu et al, 1991a), is unconcerned with the detailed flow patterns interior to the pump chamber (Affeld et al, 1976). However, fluid velocities, and hence, shear stresses and turbulent intensities, which are implicated in the mechanisms of haemolysis and thrombogenesis (Chien, 1977, Hashimoto, 1989), would be expected to increase with bulk flow rate (pump output). In this present study, these properties were investigated under a single set of pump drive conditions.

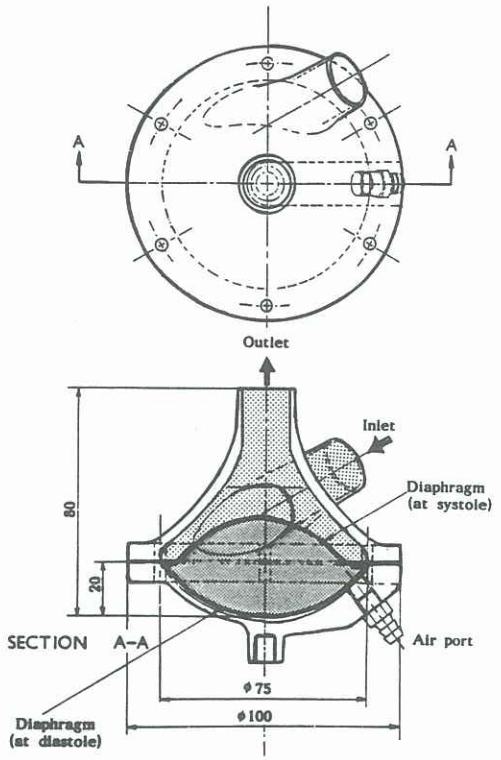

Fig. 1. Schematic Drawing of the Spiral Vortex VAD

METHOD

VAD Models

To reduce optical distortion caused by the curvature of the VAD walls, a cylindrical block of polyester was cast, reproducing the shape of the VAD on its interior surface. Thus, the model presented a normal surface to the outflow-axial viewing aspect. A diaphragm was moulded from a blend of TM5 and carbon powder, to provide a black

background to the flow field.

For comparison, a second model was constructed that featured a conventional-type (CT) VAD geometry, similar to several, commercially available models. This possessed paraxial inflow and outflow conduits, inclined at 30° to the equatorial plane.

Both models were tested with two 23-mm (tissue annulus diameter) St. Vincent's Mechanical™ heart valves fitted.

Test Circuit

The VADs were driven with a Toyobo VCT-100 computerised, pneumatic, VAD control/drive system. The pumping rate was set at 1 Hz, with a duty cycle of 3:7 dividing the drive pressure (25 kPa) and drive vacuum (-8 kPa). The preload was set to 2 kPa and the afterload to 13 kPa. Water was used as the test fluid, so flow similarity was not ideal (viscosity of blood $\approx$ 3.5 cP, density $\approx$ 1.1 g/cm^3).

Visualisation and Analysis of Flow

The flow field was investigated by the suspension method, using polystyrene particles of $\sim$ 100 μm diameter (Amberlite, Rohm & Haas Co., U.S.A.), suspended in the fluid (after soaking them in alcohol to render them neutrally buoyant), and illuminated with an obliquely-directed photographic lamp. This method provided resolution of pathlines by discrete, bright lines that resulted from the duration of the photographic exposure. Both still and cine photography were used.

A dynamic record of the motion of the tracer particles was captured on high-speed cine at framing rates of 75 Hz and 150 Hz, for which shutter speeds were 0.0089 s and 0.0044 s, respectively. The films were then transferred to video for analysis. Playback of the higher-speed record enabled qualitative assessment of the flow patterns in slow motion (ie. 20% of real-time speed), whereas hard copies of the lower-speed record (produced using a thermal, video printer) provided pathlines of sufficient length for measurement of particle velocities. Determination of the phases of the pump cycle was made by observing that the size and brightness of reflected spots from the diaphragm were maximal at the end of systole; interpolation of the tape counter reading between consecutive end-systolic phases was used to determine the relative times of frames of interest, within the cycle. Three phases of the pump cycle were examined: mid-diastole, end-diastole, and mid-systole. In each phase, 5 to 10 consecutive cycles were analysed. For each frame, particle velocities were calculated from the track lengths and grouped according to pump phase and geometric location, for statistical calculations. Then, the pathline images of all frames for a given phase were superimposed, so that the streamlines became visually apparent.

Still photographs were taken with shutter speeds from 1/30th to 1/8th s. The resulting overlap of pathlines provided an appreciation of the nature of the streamlines throughout a given phasic interval in the cycle. The shutter release of the camera was synchronised with the pump drive signal via an audible tone. Photographs were taken only at the end-diastolic phase, when particle concentration was maximal and flow accelerations were minimal (the diaphragm was not moving).

RESULTS

Slow-motion replay of the higher-speed video record provided valuable insight into the phasic development of flow patterns and velocities. With the onset of systole, a strong flow stream from the inflow tract of the SV was observed to involve the entire volume of the pump chamber, appearing to attain its highest velocities along the equator. Although the rotational speed of this vortex slowed with the end of the diastolic phase, it never approached zero; rather, it accelerated again with the onset of systole, contracting as the fluid was ejected into the outlet tract. Throughout the pump cycle, the SV exhibited mainly parallel streamlines, in contrast to the CT's disordered, turbulent flow patterns. (This phenomena is clearly visible in the still photographs, Fig. 2). Despite the emergence of a strong, early-diastolic vortex originating in the inflow tract of the CT, any trace of uniform flow or wash-

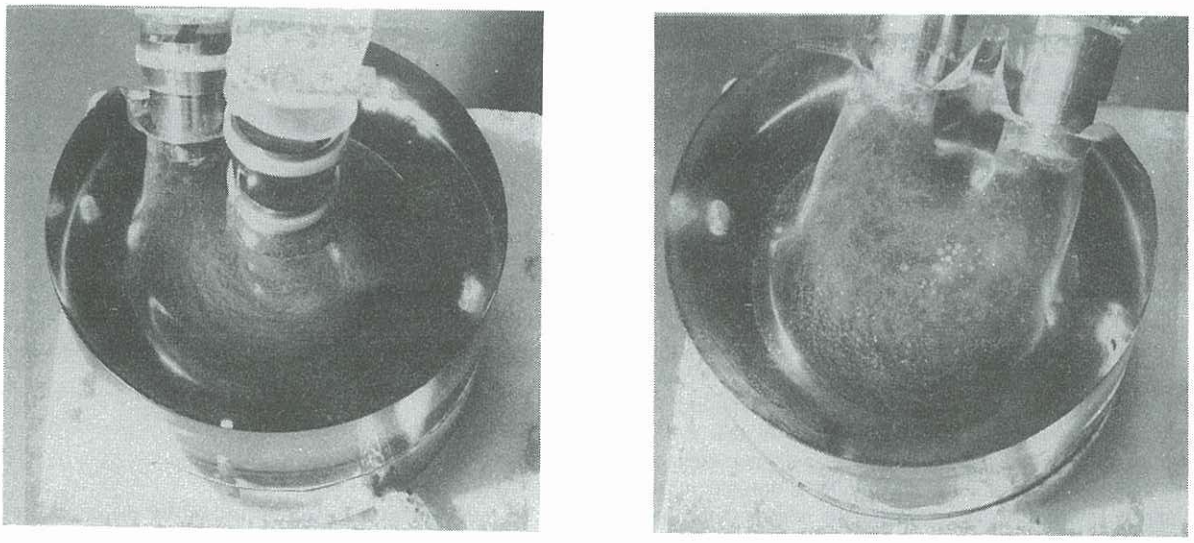

(a) Spiral Vortex (SV) VAD

(b) Conventional-type (CT) VAD

Fig. 2. Streamlines During Late-Diastole

out of the equatorial region disappeared in late diastole. Fluid velocities approached zero in some peripheral regions of the CT pump during diastole, with flow in the central region reversing direction during systole. Furthermore, little or no recirculation was apparent in the SV, whereas persistent vortices in the CT, mainly in the peripheral region between the inflow and outflow tracts, resulted in some particles remaining within the pump chamber for at least three cycles.

Quantitative analyses of frames from the slower-speed video record yielded results consistent with the qualitative observations (Table I). Mean and peak scalar flow velocities were higher in the SV (17 vs. 11 cm/s and 130 vs. 50 cm/s, respectively). The highest velocities also occurred at different phases: mid-systole for the SV, and end-diastole for the CT. Maximum shear rates in the SV and CT, which were estimated from the velocity difference between the closest, fastest moving particles, were approximately 60 s^{-1} and 20 s^{-1}, respectively, and occurred near the wall of the inflow tract, for both models (Table I).

DISCUSSION

The results revealed important differences in the fluid dynamic characteristics of the two VADs, with direct consequences for haemocompatibility. The equatorial region of blood pumps of this kind (which is also the location of the diaphragm-housing junction), is a critical region for thrombus formation (Affeld et al, 1976, Baldwin et al, 1989, Icenogle et al, 1989), which must be alleviated by providing for moderately high shear rates and good washout; the SV was found to be superior to the CT, in this regard. Furthermore, regions of flow stasis and recirculation, which also contribute to thrombosis, were eschewed by the SV, but present in the CT; this difference in behaviour between the two types of VAD has also been observed in oil-film experiments (Umezu et al, 1991b). Finally, the considerably lesser degree of turbulence that was visible in the SV suggests that this haemolytic mechanism, too, is minimised, with respect to the CT.

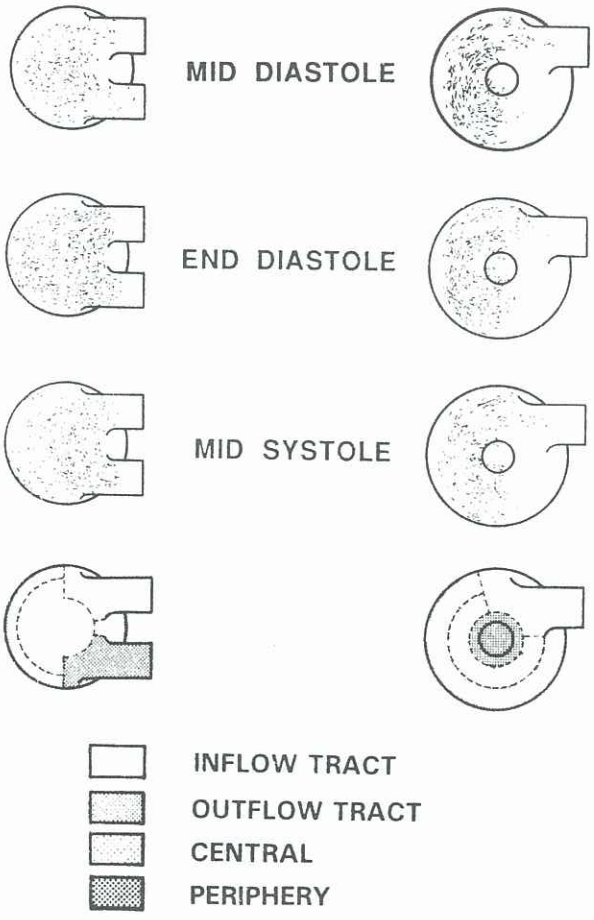

Fig. 3. Pathlines at Different Pump Phases.

Although turbulence could not be directly quantified in this study, it is possible to form some extrapolations from the measurements of fluid velocity. Because both pumps generated the same output flow rate, the higher velocities evident in the SV, versus the CT, indicates that a lesser fraction of the momentum of the SV inflow stream is converted into turbulent kinetic energy, a conclusion that is consistent with the apparent momentum-conserving character of the spiral flow. This hypothesis is further supported by the observation that in the CT, mean velocities increase later in diastole, when they should otherwise be decreasing with the deceleration of the diaphragm, and hence, the declining inflow stream velocity.

An attempt to quantify the potential for haemolysis was made by calculating shear rates, which were found to be well below the threshold for erythrocyte damage. This observation suggests that the dominant source of haemolysis within VADs is probably the Reynold's stresses, which could not be estimated in these experiments. Shear stresses would be expected to be maximal in the vicinity of the valves, and may well represent the dominant factor in the haemolytic potential of the SV, other sources having been minimised by design. Studies currently planned shall address the need for greater quantification of these parameters, and shall involve the use of laser Doppler velocimetry in a flow-similar model.

CONCLUSIONS

The design principle of the SV successfully minimises fluid dynamic parameters that are associated with haemolysis and thrombogenicity in conventional VADs.

ACKNOWLEDGEMENTS

The authors are grateful to Channel 9 Television, Sydney, for technical assistance and cine photographic services.

REFERENCES

AFFELD, K, ZARTNACK, F, MOHNHAUPT, R, BÜCHERL, ES (1976) New methods for the in vitro investigations of the flow patterns in artificial hearts. Trans Amer Soc Artif Int Organs, 22, 460-467.

BALDWIN, T, FRANCISCHELLI, D, TARBELL, J M, DEUTSCH, S, GESELOWITZ, D B (1989) Fluid mechanics of the Penn State artificial heart: LDA and dye washout studies. Proc ASME Biomechanics Symp, La Jolla, California, 257-260.

CHIEN, S (1977) Red cell membrane and hemolysis. In Cardiovascular Flow Dynamics and Measurements, HWANG N H C, NORMANN N A. ed., University Park Press, Baltimore MD, U.S.A., 757-798.

Table I. Magnitudes of Mean and Maximum Velocities (cm/s) During Different Pump Phases.

	Mid-diastole		End-diastole		Mid-systole	
	Mean	Peak	Mean	Peak	Mean	Peak
CT						
Inflow tract	10	24	13	48	10	36
Periphery	13	48	12	36	11	36
Central	10	36	13	48	9	36
Outflow tract	10	36	12	36	12	36
Overall	10	48	13	48	10	36
SV						
Inflow tract	16	85	13	61	22	130
Periphery	22	61	17	61	18	61
Central	18	61	12	37	15	85
Outflow tract	15	49	15	61	16	49
Overall	18	85	15	61	17	130

FARRAR, D J, HILL, J D, LAMAN, M D, GRAY, A, PENNINGTON, G D, MCBRIDE, L R, PIERCE, W S, PAE, W E, GLENVILLE, B, ROSS, D, GALBRAITH, T A, ZUMBRO, G L (1988) Heterotopic prosthetic ventricles as a bridge to cardiac transplantation. New England J Med, 318, 333-340.

HASHIMOTO, S (1989) Erythrocyte destruction under periodically fluctuating shear rate: comparative study with constant shear rate. Artif Organs, 13, 458-463.

ICENOGLE, T B, SMITH, R G, CLEAVINGER, M, VASU, M A, WILLIAMS, R J, SETHI, G K, COPELAND, J C (1989) Thromboembolitic complications of the Symbion AVAD system, Artif Organs, 13, 532-539.

UMEZU, M, YE, C-X., NUGENT, A.H., CHANG, V.P. (1991a) Preliminary study - optimisation of the Spiral Vortex blood pump. In Artifical Heart 3, T. Akutsu, H. Koyanagi, ed., Springer-Verlag, Tokyo, Japan, 107-116.

UMEZU, M, YE, C-X., NUGENT, A.H., CHANG, V.P. (1991b) The advantages of the Spiral Vortex design in pneumatic blood pumps as demonstrated by dye-washout tests. Artif Organs, 14 (Suppl 4), 31-33.